Heliyon 10 (2024) e35404

Contents lists available at ScienceDirect

Heliyon

journal homepage: www.cell.com/heliyon

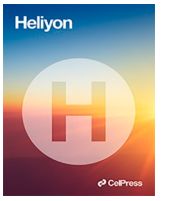

Research article

A pan-cancer cuproptosis signature predicting immunotherapy response and prognosis

Xiaojing Zhu, Zixin Zhang, Yanqi Xiao, Hao Wang, Jiaxing Zhang, Mingwei Wang, Minghui Jiang, Yan Xu *

College of Bioinformatics Science and Technology, Harbin Medical University, Harbin, China

A R T I C L E I N F O

Keywords:
Cuproptosis
Prognosis
Immunotherapy
Machine learning
Pan-cancer

A B S T R A C T

Background: Cuproptosis may represent a potential biomarker for predicting prognosis and immunotherapy response, but the available evidence is insufficient.
Methods: The multiple single-cell RNA sequencing (scRNA-seq) datasets were analyzed to investigate the specific occurrence of cuproptosis in distinct cell populations. Utilizing 28 scRNA-seq datasets, TCGA pan-cancer cohort, and 10 immunotherapy cohorts, we developed a cuproptosis signature (Cup.Sig). This signature was used to construct prediction models for immunotherapy response and identify potential prognostic biomarkers for pan-cancer using 11 different machine learning algorithms.
Results: Malignant cells demonstrate the higher cuproptosis scores in comparison to other cell types across diverse cancer types. The Cup.Sig exhibits significant associations with cancer hallmarks and immune cell response in multiple cancer types. Leveraging the Cup.Sig, the robust pan-cancer immunotherapy prediction model and prognostic biomarker have been established and validated using diverse datasets from various platforms.
Conclusions: We developed a pan-cancer cuproptosis signature for predicting survival and immunotherapy response.

1. Introduction

Copper, a trace element present in the human body, plays a pivotal role in diverse signaling pathways and biological processes [1]. However, excessive levels of copper can trigger cell death [2]. The independent nature of copper-induced cell death has been subject to extensive argued until recent discoveries shed light on its mechanism: copper-mediated cell death is now acknowledged as an independent form closely associated with mitochondrial respiration and lipoic acid (LA) pathway [3]. The impact of cuproptosis resulting from disrupted copper homeostasis in tumor cells on patient prognosis and resistance to treatment remains uncertain. Therefore, in the realm of precision oncology, targeting cuproptosis in tumor cells holds great potential as a means for predicting survival outcomes and evaluating the effectiveness of immunotherapy.

Considering the close correlation between cuproptosis and cellular metabolism, as well as the observed elevated levels of aerobic respiration in various cancers such as breast cancer, Skin Cutaneous Melanoma (SKCM), and leukemia [4,5], an increasing number of studies are currently focusing on investigating the intricate association between cuproptosis and cancer [6–8]. On one hand, the

* Corresponding author.
E-mail address: xuyan@ems.hrbmu.edu.cn (Y. Xu).

https://doi.org/10.1016/j.heliyon.2024.e35404
Received 15 February 2024; Received in revised form 26 July 2024; Accepted 29 July 2024
Available online 30 July 2024

prognostic significance of cuproptosis genes in cancer has been extensively investigated. For example, in various cancer types, genes associated with cuproptosis, such as DLD [9], DLAT [10], and LIAS [11], are considered significant factors influencing tumor prognosis. Furthermore, besides individual gene analysis, certain studies have also investigated the correlation between cuproptosis and tumor prognosis by integrating these specific genes to construct risk mode [12,13]. These genes exhibit diverse functions in various tumor types, thereby complicating the assessment of tumor prognosis based on cuproptosis-related genes. The determination of their potential prognostic impacts necessitates more comprehensive mechanistic research and analysis across multiple omics levels. Moreover, certain malignant tumors, such as SKCM, breast cancer, leukemia, glioblastoma, and cholangiocarcinoma (CHOL), exhibit augmented mitochondrial metabolism [5,10,14]. Drug-resistant tumors also demonstrate heightened mitochondrial metabolic status [15,16]. In addition to tumor metabolism, a correlation between cuproptosis and tumor immunity has been observed [17]. Notably, investigations have focused on immune checkpoint genes such as PD-1 that are associated with tumor immune suppression and immunotherapy. These studies have revealed significant variations in the expression of these genes among groups with high or low scores of cuproptosis-related signatures across different types of cancer [18–20]. Furthermore, multiple analyses examining differential gene enrichment between different cuproptosis-related groups have demonstrated close associations with both metabolism and immunity-related genes [18,21]. The strong correlation observed between cuproptosis and levels of mitochondrial metabolism and immunity underscores the potential significance of cuproptosis in predicting the effectiveness of anticancer therapies and devising strategies for cancer treatment.

In this study, we utilized extensive pan-cancer single-cell and bulk RNA sequencing datasets to identify genes associated with cuproptosis, a crucial factor in cancer biology known for its involvement in treatment resistance. Moreover, by employing diverse machine learning techniques, we developed predictive models that utilize these genes to predict survival outcomes and predict response to immune therapy. These findings highlight the potential of these identified genes as targets for prognosticating survival outcomes and predicting immunotherapy response.

2. Methods

2.1. Acquisition and processing of pan-cancer single-cell RNA sequencing (scRNA-seq) datasets

To investigate the cuproptosis in the tumor microenvironment and develop cuproptosis-related signature (Cup.Sig), we obtained a total of 28 scRNA-seq datasets and annotation information from the Tumor Immune Single-cell Hub 2 (TISCH2) portal website (http://tisch.comp-genomics.org/) [22]. The dataset encompasses malignant cells, stromal cells, and immune cells obtained from 379 patients, amounting to a total of 1,182,774 individual cells. These datasets encompass diverse cancer types, including Basal Cell Carcinoma (BCC), Colorectal Cancer (CRC), CHOL, Diffuse Large B-Cell Lymphoma (DLBC), Esophageal Cancer (ESCA), Glioblastoma, Head and Neck Squamous Cell Carcinoma (HNSC), Liver Hepatocellular Carcinoma (LIHC), Merkel Cell Carcinoma (MCC) , Multiple Myeloma (MM) , Nasopharyngeal Carcinoma (NPC) , Non-Small Cell Lung Cancer (NSCLC), Ovarian Serous Cystadenocarcinom (OV), Pancreatic Ductal Adenocarcinom (PAAD) and Prostate Adenocarcinom (PRAD). Please refer to Table S1 for detailed information. The datasets underwent quality control and clustering procedures following the guidelines provided in the tutorial of the R package 'Seurat' [23]. We also utilized the R package Seurat to identify differentially upregulated genes in malignant cells within each dataset, employing a threshold of log-fold change (logFC) ≥ 0.25 and false discovery rate (FDR) < 0.05. We used the "irGSEA.score" function from the irGSEA package (https://github.com/chuiqin/irGSEA), employing the "ssgsea" method parameter, to ascertain the cellular cuproptosis scores in each dataset based on the expression of cuproptosis-related genes including *FDX1*, *DLD*, *DLAT*, *PDHA1*, *PDHB*, *MTF1*, *GLS*, *CDKN2A*, *DBT*, *ATP7A*, and *DLST* [24].

2.2. Processing of pan-cancer bulk RNA-seq datasets

To explore the correlation between Cup.Sig score, evaluated by GSVA, and cancer hallmarks, tumor immune infiltration, and survival outcomes across various cancer types, we downloaded gene expression and clinical data of the Cancer Genome Atlas (TCGA) pan-cancer cohort from the UCSC Xena Data Portal (https://xenabrowser.net) [25], exclusively selecting samples with survival information for subsequent analysis. Furthermore, we obtained total mutation burden (TMB) data for TCGA pan-cancer samples from cBioPortal (https://www.cbioportal.org) [26], and acquired intratumor heterogeneity (ITH) data from a study conducted by Torsson et al. [27], which used to analyze the correlation between Cup.Sig and TMB or ITH. To validate the prognostic value of the Cup.Sig-related risk score, we retrieved gene expression and clinical data for breast cancer from cBioPortal (https://www.cbioportal.org) [28]. Additionally, we obtained gene expression data and survival information for liver hepatocellular carcinoma (HCC) patients from International Cancer Genome Consortium (ICGC) Data Portal (https://dcc.icgc.org/). Furthermore, clinical and survival information for various cancer types was acquired from the Gene Expression Omnibus (GEO; https://www.ncbi.nlm.nih.gov/geo/) database, including GSE42568 (BRCA) [29], GSE41258 (COAD) [30], GSE65858 (HNSC) [31], GSE2748 (KIRP) [32], GSE140901 (LIHC) [33], GSE31210 (LUAD) [34], GSE11969 (Lung cancer) [35], GSE61676 (NSCLC) [36] and GSE21501 (PDAC) [37]. The comprehensive details regarding these datasets can be accessed in Table S2.

2.3. Acquisition and processing of immune checkpoint inhibitor (ICI) RNA-Seq cohorts

We obtained gene expression data and prognosis information from cohorts of immune therapy targeting programmed cell death ligand 1 (PD-L1)/programmed cell death protein 1 (PD-1) or cytotoxic T lymphocyte-associated antigen 4 (CTLA-4). These cohorts

consisted of six SKCM cohorts (SKCM Gide 2019 [38], SKCM Nathanson 2017 [39], SKCM Liu 2019 [40], SKCM Hugo 2016 [41], SKCM VanAllen 2015 [42] and SKCM Riaz 2017 [43]), one urothelial carcinoma cohort (UC Mariathasan 2018 [44]), one glioblastoma cohort (GBM Zhao 2019 [45]), one gastric cancer cohort (STAD Kim 2018 [46]), and one renal cell carcinoma cohort (RCC Braun 2020 [47]). Only treatment-naïve patients were included for further analysis. Among them, complete remission (CR) and partial remission (PR) were categorized as treatment responders, whereas stable disease (SD) and progressive disease (PD) were deemed non-responders. All processed data for the immune therapy cohorts were acquired from GEO or corresponding published online articles (Table S3).

2.4. Functional and pathway enrichment analysis

The GSVA method from the R package was utilized to perform gene set variation analysis on 50 signature gene sets obtained from molecular signature databases (https://www.gsea-msigdb.org/gsea/msigdb), along with the Cup.Sig gene set. Additionally, gene ontology (GO) analysis was conducted using the clusterProfiler R package [48]. Pathways for which the p.adj was <0.05 were considered significantly enriched.

2.5. Analysis of immune infiltration

The Cell-type Identifcation by Estimating Relative Subsets of RNA Transcripts (CIBERSORT) algorithm and LM22 signature matrix were employed to estimate immune cell infiltration based on transcriptome data from the TCGA pan-cancer cohort [49]. The stromal and immune cells within malignant tumor tissues (ESTIMATE) were utilized to assess four indicators, comprising of immune score, stromal score, ESTIMATE score, and tumor purity. These assessments were based on expression data obtained from the TCGA pan-cancer cohort samples. The Immune Score reflects the quantity and activity level of immune cells in tumor tissue. Stromal Score reflects the quantity and types of non-malignant cells in tumor tissue. ESTIMATE score comprehensively considers both Immune Score and Stromal Score to provide a comprehensive assessment of the tumor microenvironment. Tumor purity refers to the relative proportion of malignant tumor cells in tumor tissue.

2.6. Developing a machine learning-based model for predicting the response to immune checkpoint blockade

To investigate the predictive ability of Cup.Sig for ICI therapy response, we curated transcriptome sequencing data and clinical outcomes from 10 immunotherapy cohorts (Table S3). Initially, we integrated five immunotherapy datasets into a comprehensive dataset ($n = 775$), comprising SKCM Gide 2019 ($n = 91$), RCC Braun 2020 ($n = 281$), SKCM Nathanson 2017 ($n = 24$), SKCM Liu 2019 ($n = 121$), and STAD Kim 2018 ($n = 78$). Subsequently, we employed the 'ComBat' function in the R package sva to effectively correct batch effects across different datasets [50]. Following this, the merged dataset was randomly partitioned into a training set (80 %) and a validation set (20 %). We employed ten machine learning algorithms, namely gbm, KKNN, pam, rf, lda, AdaBoost, Adabag, freebag, slad and glmnet, based on Cup.Sig to construct prediction models on the training set. All classification algorithms were implemented using the 'Caret' package in R and underwent five repeated ten-fold cross-validations to validate model performance. To ensure the robustness of our findings, we performed ten iterations of the optimization process by employing unique random seed. Finally, these ten models were applied to the validation set and their performances were compared in order to select the model with the highest accuracy as the final classification model. In addition, we assessed the predictive performance of our final model on five independent test sets: GBM Zhao 2019 ($n = 34$), SKCM Hugo 2016 ($n = 26$), SKCM VanAllen 2015 ($n = 153$), SKCM Riaz 2017 ($n = 105$), and UC Mariathasan 2018 ($n = 298$). Furthermore, we compared predictive capabilities of Cup.Sig with two other pan-cancer immune therapy response prediction signatures (NFG.Sig [51] and NLRP3.Sig [52]) across these five cohorts.

2.7. Development and validation of the Cup.Sig-related prognostic risk score

We performed LASSO (Least Absolute Shrinkage and Selection Operator) regularized regression analysis on the 125 features of Cup.Sig. Ten-fold cross-validation was employed to identify a subset of features that demonstrated the strongest correlation with overall survival in the TCGA cancer cohort. The 'glmnet' package in R language was utilized for implementing LASSO regularization regression. Subsequently, we developed a multivariate Cox proportional hazards regression model using a stepwise approach based on the overall survival data from the TCGA pan-cancer training set ($n = 80$ %). Based on this model, individualized risk scores related to Cup.Sig were computed for each patient by multiplying gene expression levels with their corresponding Cox regression coefficients. Using this formula, we calculated risk scores for each patient in the TCGA pan-cancer training set, TCGA pan-cancer validation set, and external validation set. Subsequently, patients were categorized into high-risk and low-risk groups based on optimal cutoff values. Differences in overall survival were then analyzed utilizing the 'survival' R package. We employed univariate Cox regression analysis to assess the prognostic value of the Cup.Sig risk score for overall survival (OS), progression-free interval (PFI), and disease-specific survival (DSS).

2.8. Statistical analysis

All statistical analyses were conducted using the R software. Kaplan-Meier curves and log-rank tests were employed to evaluate the survival disparities between the two groups. Univariate and multivariate Cox regression analyses were utilized to identify prognostic

factors. Pearson's method was applied for correlation analysis of normally distributed data, while Spearman's method was used for non-normally distributed data. A significance level of p and p.adj <0.05 was considered statistically significant.

3. Result

3.1. The cuproptosis scores of malignant cells within the tumor microenvironment are enhanced

To evaluate the cuproptosis status of distinct cellular subpopulations within the tumor microenvironment, we collected four

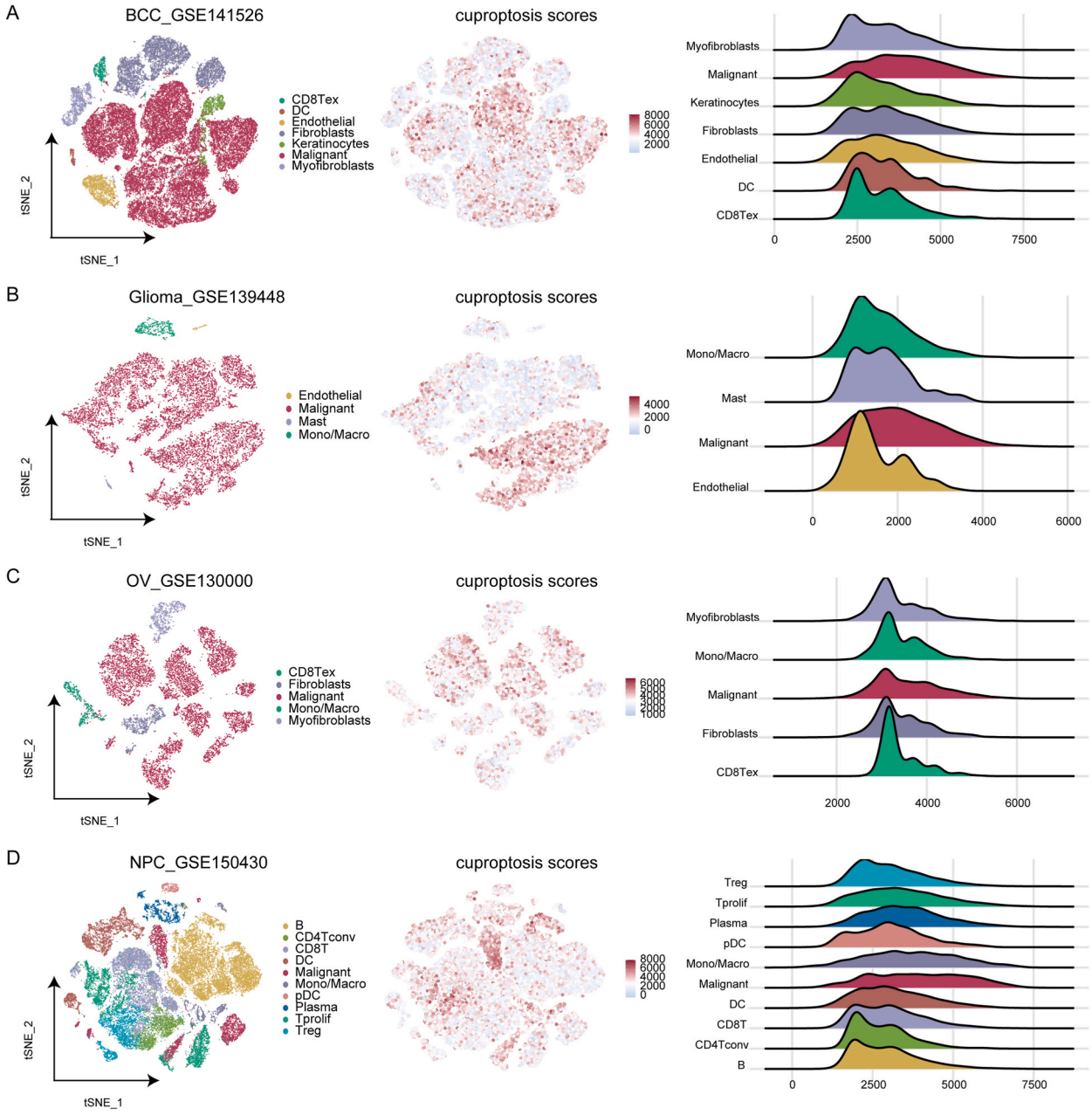

Fig. 1. Evaluation of cuproptosis scores for individual cell types in the tumor microenvironment. The t-SNE plots demonstrate the clustering of cells and provide annotation results for different scRNA-seq datasets representing various tumor entities (A-D, left). The feature plots depict enrichment scores of gene sets associated with cuproptosis in each specific cell type (A-D, middle). The ridge plots (A-D, right) illustrate the distribution of cuproptosis scores within distinct cell populations. Mono/Macro Monocytes and macrophages, DC Dendritic cells, pDC plasmacytoid DCs, CD8Tex Exhausted CD8 T cells.

publicly available single-cell RNA sequencing (scRNA-seq) datasets encompassing BCC, glioma, OV, and NPC. Subsequently, we utilized a set of 11 cuproptosis-associated genes to calculate a cellular cuproptosis score. We extract and cluster high-quality cells from all datasets, and annotating them based on their original cell labels (Fig. 1A–D; left). It was observed that malignant cells exhibit higher cuproptosis scores compared to other cellular components within the microenvironment, including myeloid cells, T cells, B cells, and endothelial cells (Fig. 1A–D; middle and right). These findings imply that malignant cells may consistently exhibit a dysregulation in

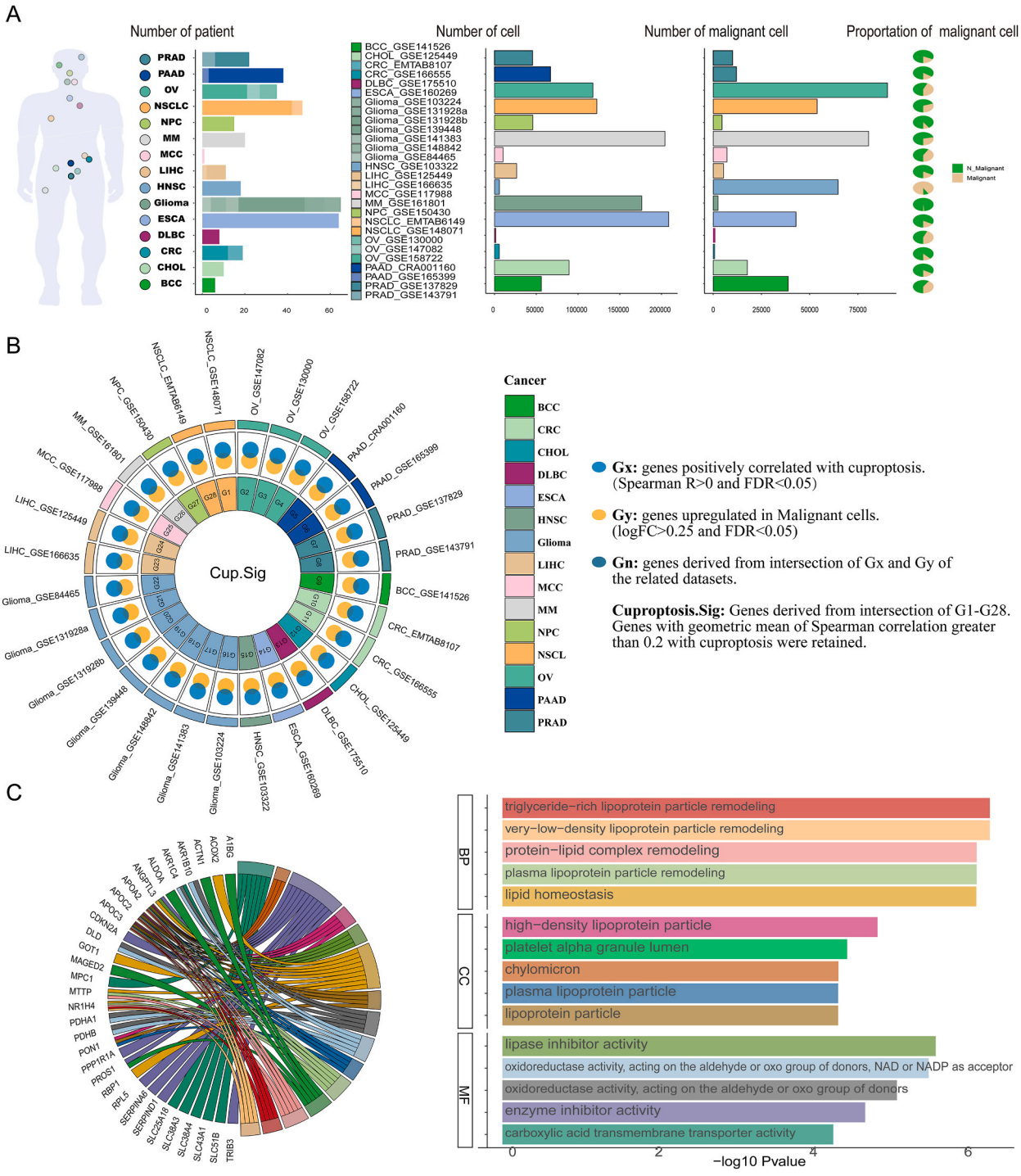

Fig. 2. Development and description of cuproptosis signature (Cup.Sig). (A) An overview of the origin of the patient cohort and the corresponding number of patients, cells, malignant cells, and proportion of malignant cells for 15 types of cancer from left to right. (B) Circus plot depicting the development of Cup.Sig. (C) Enrichment analysis of genes associated with Cup.Sig.

copper homeostasis within the tumor microenvironment across diverse cancer types. Given these results, we hypothesize that transcriptional alterations associated with cuproptosis in malignant cells could serve as potential biomarkers for predicting survival outcomes and response to immune therapy in cancer patients.

3.2. Development of a malignant cuproptosis signature (Cup.Sig) through scRNA-seq analysis across multiple cancer types

Our objective is to establish a gene signature that specifically reflects the distinctive cuproptosis characteristics exhibited by malignant cells across various types of cancer. To accomplish this objective, we utilized a total of 28 datasets from single-cell RNA sequencing, encompassing 15 different cancer types (Fig. 2A; Table S1). These datasets were employed to perform Spearman correlation analysis between gene expression levels in malignant cells and cuproptosis scores. In these 28 datasets, genes exhibiting a positive correlation with the cuproptosis score (Spearman R > 0 and FDR<0.05) were considered as "Gx", indicating their linkage to cuproptosis. Genes that demonstrated upregulation in malignant cells (logFC≥0.25 and FDR<0.05) were designated as "Gy", representing specific malignant cell genes. To identify the specific cuproptosis-regulating genes in malignant cells, we determined the intersection of "Gx" and "Gy" to generate "Gn" (n = 1–28) for each dataset, denoting the common genes between Gx and Gy across all 28 scRNA-Seq datasets. Subsequently, we calculated the geometric mean Spearman correlation coefficient for each gene from G1 to G28. Finally, we selected genes with a geometric mean Spearman correlation coefficient greater than 0.2, resulting in Cup.Sig comprising 125 genes (Fig. 2B; Table S4). We conducted further analysis on the biological functions regulated by Cup.Sig and observed its

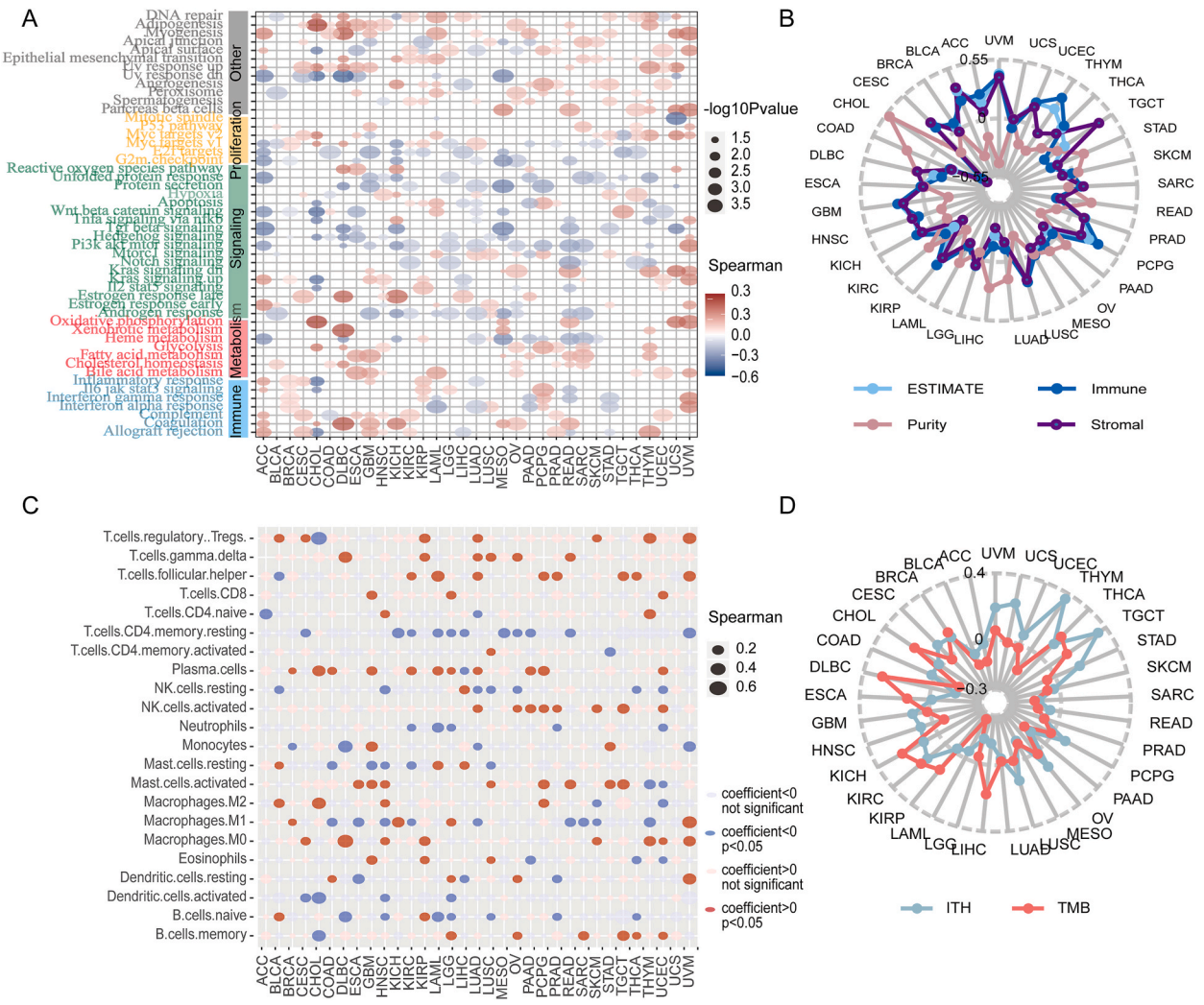

Fig. 3. Pan-cancer analysis of Cup.Sig across 33 cancer types in the TCGA cohort. (A) The association between Cup.Sig scores and enrichment scores of cancer hallmark pathways, where blue dots represent negative correlation and red dots indicate positive correlation. (B) Summary of the relationship between Cup.Sig scores and tumor purity, immune, stromal, and ESTIMATE scores. (C) Correlation analysis between Cup.Sig scores and immune infiltration (CIBERSORT), with blue dots indicating negative correlation and red dots indicating positive correlation. (D) Correlation analysis between Cup.Sig scores and TMB/ITH.

predominant enrichment in metabolism-related processes, specifically encompassing triglyceride-rich lipoprotein particle remodeling, high-density lipoprotein particle, and lipase inhibitor activity (Fig. 2C). This finding aligns with previous research indicating that disruptions in copper homeostasis can perturb metabolic pathways and induce cuproptosis [2].

3.3. Analyzing the potential association between Cup.Sig and cancer hallmarks, and immune cell infiltration in the TCGA pan-cancer cohort

To further investigate the biological characteristics of Cup.Sig in cancer, we employed the GSVA method to calculate Cup.Sig scores for each patient within the TCGA 33-cancer cohort. We conducted further analysis on the correlation between Cup.Sig scores and cancer hallmark enrichment scores in the TCGA pan-cancer cohort (Fig. 3A). As anticipated, Cup.Sig scores exhibited a significant positive correlation with multiple metabolism-related pathways across various cancers. Conversely, certain signaling and proliferation-related pathways displayed a negative association with Cup.Sig scores. Notably, at the pan-cancer level, we also observed a significant relationship between Cup.Sig scores and immune-related pathways, indicating a potential connection between Cup.Sig and immune cell infiltration within the tumor microenvironment (Fig. 3B). The ESTIMATE results additionally confirmed a substantial association between Cup.Sig scores and both immune scores as well as ESTIMATE across multiple cancer types. Furthermore, the evaluation of the TCGA pan-cancer cohort using CIBERSORT revealed a significant association between Cup.Sig score and alterations in tumor-infiltrating immune cells (Fig. 3C). For instance, across various cancer types, there was a positive correlation observed between Cup.Sig score and activated NK cells, while a negative correlation was found with resting CD4 memory T cells. In addition, we analyzed the correlation between Cup.Sig score and ITH, a feature that mediates immunosuppression [53], as well as known immune-related factor tumor mutational burden (TMB) (Fig. 3D). The results showed a significant correlation between Cup.Sig score and ITH/TMB in various cancers within the TCGA pan-cancer cohort, further confirming the close association between Cup.Sig score and tumor immunity. In conclusion, we established a malignant cells-specific, cuproptosis-related transcriptomic signature that exhibits close associations with various cancer hallmark pathways and immune cell imbalances, suggesting its potential as a predictive

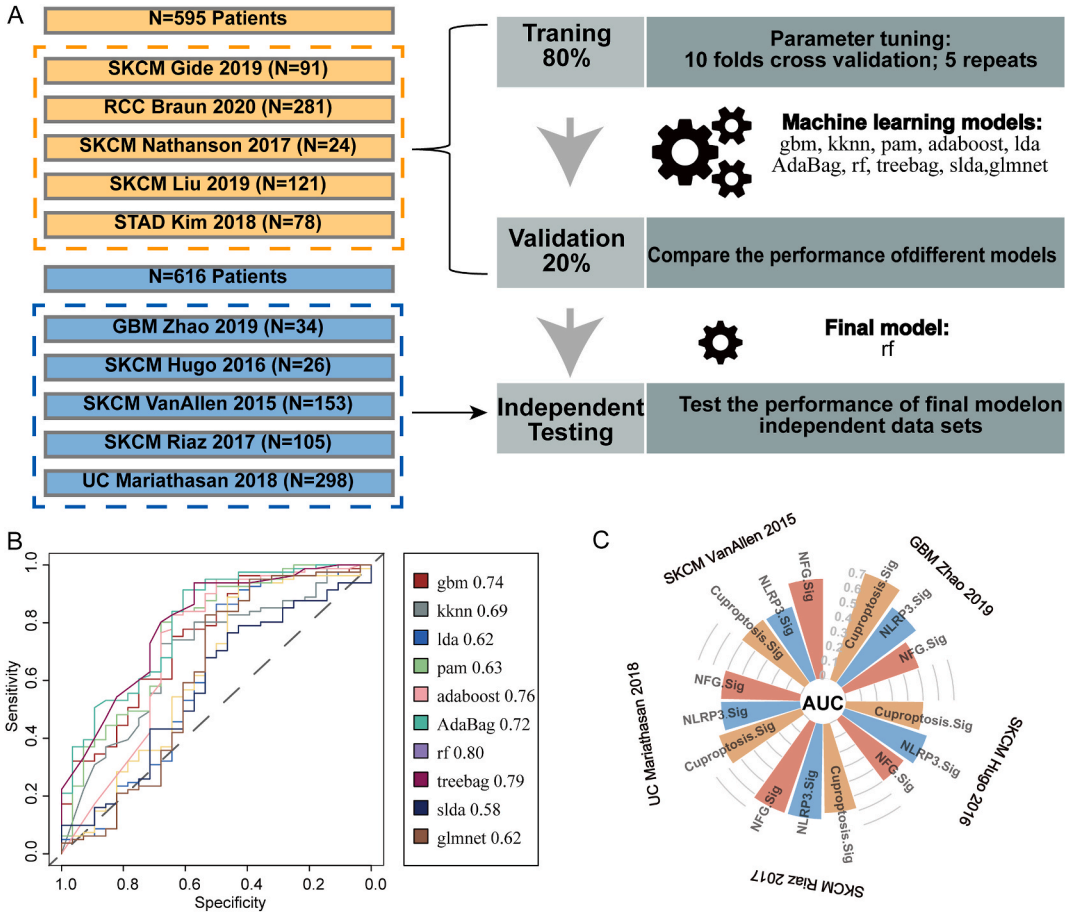

Fig. 4. Using Cup.Sig to predict the outcome of immunotherapy. (A) The process description of constructing a Cup.Sig immunotherapy response prediction model based on various machine learning algorithms. (B) The receiver operating characteristic (ROC) curve demonstrates the performance of different machine learning algorithms in the validation set. (C) The ROC curve compares the performance of the final Cup.Sig model with two previously published pan-cancer models for response to immunotherapy in the validation set.

factor for pan-cancer immune response.

3.4. Prediction of immunotherapy outcome using Cup.Sig

Based on the observed correlation between Cup.Sig scores and imbalanced infiltration of immune cells in tumors, as well as their association with robust predictors of pan-cancer response to anti-PD-L1/PD-1 immunotherapy such as TMB, we further hypothesize that Cup.Sig could potentially serve as predictive indicators for the response to immune checkpoint inhibitor therapy. We first evaluated the Cup.Sig scores of malignant cells in the single-cell RNA sequencing dataset GSE123813 from patients with basal cell carcinoma (BCC) undergoing immunotherapy, and found that malignant cells from immunotherapy-resistant patients exhibited significantly higher Cup.Sig scores (Fig. S1). Next, to predict the outcomes of PD-L1/PD-1 or anti-CTLA-4 immunotherapy based on Cup.Sig, we curated 10 bulk RNA-seq datasets comprising immunotherapy results (Fig. 4A). Among these cohorts, we integrated 5 (n = 595) and divided them into a training set (80 %) and a validation set (20 %). The remaining 5 cohorts were utilized for testing the predictive capacity of the final model. Subsequently, we employed 10 distinct machine learning algorithms and conducted repeated 10-fold cross-validation for each model to optimize parameters. We then assessed the area under curve (AUC) values of these models in the validation cohort. Through this series of computations, we ultimately selected an "rf" machine learning algorithm model with a maximum AUC value reaching up to 0.8 (Fig. 4B). We further compared the performance of the Cup.Sig prediction model with previously established pan-cancer predictive models for anti-PD-L1/PD-1 or anti-CTLA-4 immunotherapy response (including NLRP3.Sig and NFG.Sig). We found that these two pan-cancer prediction models performed well only on a single dataset, while the Cup.Sig prediction model performed well across multiple cohorts covering various cancer types such as SKCM, GBM, and UC. Specifically, NLRP3.Sig achieved only 0.62 in the SKCM Riaz 2017 cohort, with AUC values dropping to around 0.5 in the UC Mariathasan 2018 and SKCM VanAllen 2015 cohorts. NFG.Sig performed well in the UC Mariathasan 2018 and SKCM Riaz 2017 cohorts but showed poorer performance in the other three cohorts (Fig. 4C). In contrast, the Cup.Sig prediction model demonstrated good performance across all cohorts, it was observed that all five external cohorts exhibited AUC values greater than 0.5 and achieved a maximum value of 0.73 (Fig. 4C). In conclusion, these results indicate that Cup.Sig has the potential to serve as a reliable pan-cancer predictive model for response to PD-L1/PD-1 or CTLA-4 immune therapy.

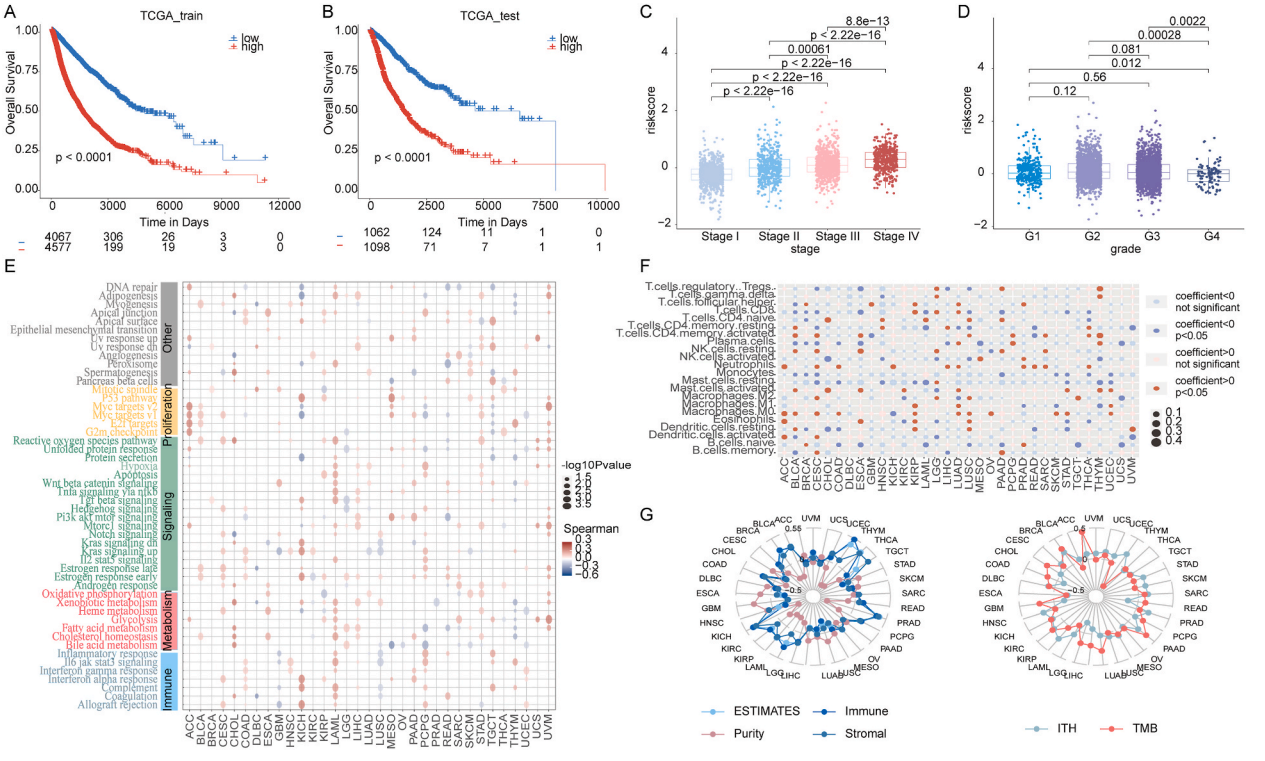

Fig. 5. The predictive performance of the Cup.Sig-related pan-cancer prognosis risk score in the TCGA cohort. (A, B) Kaplan-Meier analysis showed the association between Cup.Sig-related risk scores and overall survival (OS) in both training and testing sets of patients. (C, D) Revealed differences in Cup.Sig-related risk scores among different tumor stages and grades. (E) Demonstrated correlations between Cup.Sig-related risk scores and cancer hallmark pathway enrichment across 33 cancer types. (F) Showed association between Cup.Sig-related risk scores and abundance of 22 immune cell infiltrates across 33 cancer types. (G) Demonstrated association between Cup.Sig-related risk scores and TMB/ITH.

3.5. Construction and validation of a pan-cancer prognostic model related to Cup.Sig

Next, we performed univariate Cox analysis on 33 types of cancer in TCGA, and the results showed that each gene associated with Cup.Sig was significantly correlated with patient prognosis in at least two types of cancer (Fig. S2). Therefore, we attempted to examine the predictive capacity of Cup.Sig on patient survival outcomes in a pan-cancer cohort. We optimized Cup.Sig through implementation of the LASSO penalized Cox proportional hazards regression (LASSO-Cox) model. Specifically, we initially incorporated Cup.Sig genes into the TCGA pan-cancer cohort for LASSO analysis and conducted 10-fold cross-validation to identify 63 significant genes (Table S5). Subsequently, utilizing the expression values and coefficients of these 63 genes, we computed risk scores for each patient within the TCGA pan-cancer training set (Fig. 5A). Ultimately, based on these risk scores, patients from both the TCGA training and testing sets were stratified into two groups. Our findings revealed that individuals with higher risk scores in both cohorts exhibited poorer overall survival rates (Fig. 5B, $p < 0.05$, log-rank test). The patients with higher clinical stages and grades also displayed significantly higher risk scores (Fig. 5C and D, $p < 0.05$, Wilcoxon rank-sum test). The multivariate Cox regression analysis also observed that these Cup.Sig related prognosis model genes were significantly associated with patient OS (Fig. S3). Furthermore, correlation coefficients between cancer hallmark GSVA scores and Cup.Sig-related risk scores were calculated (Fig. 5E). We found that in the TCGA cohort, Cup.Sig-related risk scores for various cancers were positively correlated with tumor-promoting pathways such as hypoxia, epithelial-mesenchymal transition (EMT), and Wnt β signaling as indicated by GSVA scores. Moreover, immune infiltration analysis showed a significant association between Cup.Sig-related risk scores and immune infiltration as well as tumor heterogeneity within the TCGA pan-cancer cohort (Fig. 5F and G). We also observed a significant predictive ability for overall survival in 24 types of cancer in TCGA when considering Cup.Sig-related risk scores (Fig. S4, $p < 0.05$, log-rank test). To further validate the prognostic value of this risk score, in the TCGA pan-cancer cohort, we performed a comprehensive univariate Cox analysis by integrating Disease Specific Survival (DSS), Progression Free Interval (PFI), and OS to assess risk scores (Fig. 6A). Our findings revealed a significant correlation between the Cup.Sig-related risk score and compromised survival across diverse cancer types. Furthermore, we applied the same formula to calculate the risk scores in several external validation cohorts. These datasets demonstrated that Cup.Sig-related risk scores also exhibited strong performance in predicting patient survival, thereby confirming the reliability of Cup.Sig as a prognostic indicator across various cancers (Fig. 6B–L, $p < 0.05$, log-rank test).

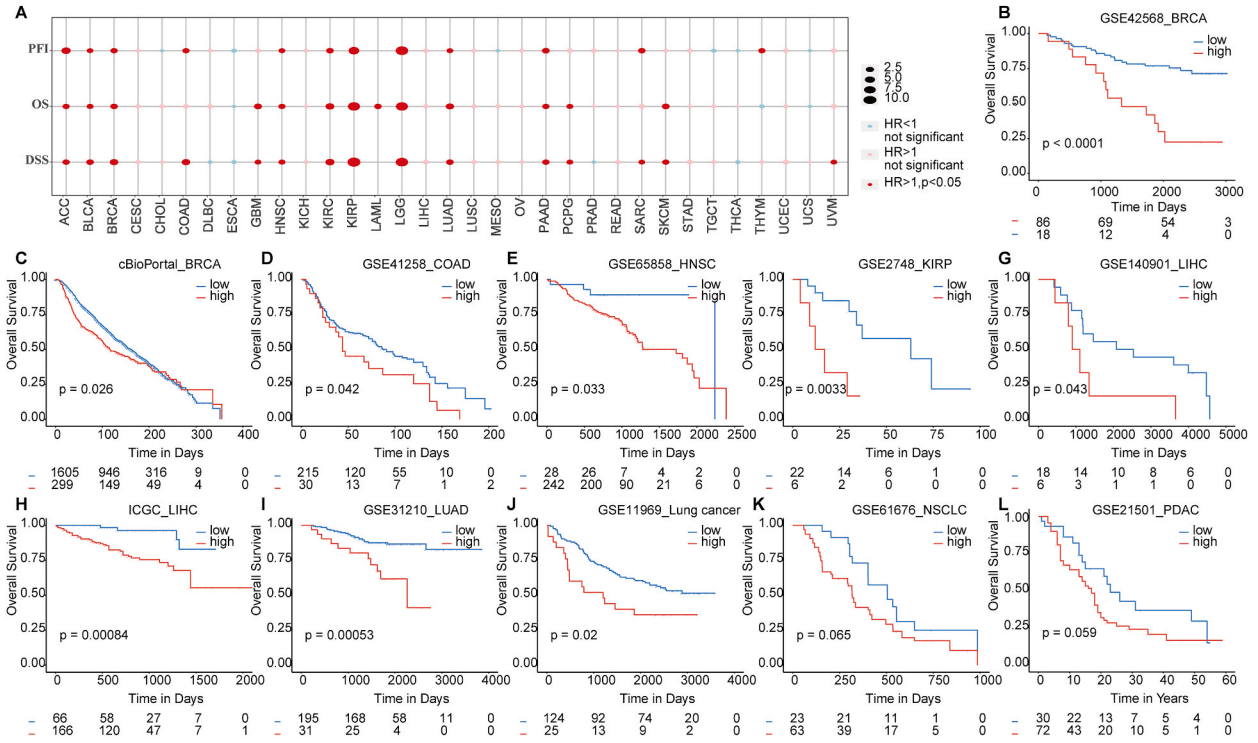

Fig. 6. The prognostic performance of Cup.Sig-related pan-cancer model in TCGA and external cohorts. (A) Univariate analysis of the association between patient Cup.Sig-related risk scores and OS, PFI, and DSS in the TCGA cohort. (B–L) The risk scores and OS Kaplan-Meier analysis of patients in the external cohorts encompass GSE42568_BRCA, cBioPortal_BRCA, GSE41258_COAD, GSE65858_HNSC, GSE2748_KIRP, GSE140901_LIHC, ICGC_LIHC, GSE31210_LUAD, GSE11969_Lung cancer, GSE61676_NSCLC and GSE21501_PDAC cohorts.

4. Discussion

Although the involvement of copper-induced cell death in cancer signaling pathways and tumor characteristics has been established [1,54], there remains a dearth of studies investigating its impact on overall cancer prognosis and immunomodulatory response. Here, we assessed the cuproptosis scores of diverse cell types within the tumor microenvironment across multiple cancer types at a single-cell level, based on cuproptosis-related genes. Our findings demonstrated that malignant cells exhibited elevated cuproptosis scores in various cancers. Next, we collected 28 datasets encompassing 15 cancer types and developed a novel pan-cancer malignant cell cuproptosis signature (Cup.Sig). In the TCGA pan-cancer cohort, we observed strong associations between Cup.Sig and tumor signaling pathways as well as characteristics. Leveraging different machine learning techniques, we established pan-cancer models for predicting response to ICI therapy and prognosis using Cup.Sig. Finally, external validation of these models was performed utilizing distinct datasets from multiple platforms.

The cuproptosis genes have been extensively documented for their pivotal role in the regulation of tumor occurrence and progression. For instance, the core regulatory gene *DLD* exhibites different expression in most cancers. Furthermore, survival analysis indicates that *DLD* is correlated with both overall survival and progression-free survival in tumors, potentially impacting the prognosis of cancer patients [55]. In addition, *CDKN2A* has the highest mutation frequency in all tumors in TCGA, and is associated with poor prognosis in cancer patients [56]. Recent studies have also identified *PDHA1* as a potential prognostic and immune-related biomarker in various cancer types [57]. We observed a higher cuproptosis score at the single-cell level in malignant cells within the tumor microenvironment, which is consistent with previously reported significantly elevated levels of copper ions in the serum of patients diagnosed with lung cancer [58], prostate cancer [59], breast cancer [60], gastric cancer [61], and thyroid cancer [62]. Similarly, studies have also identified an increase in copper ions within gallbladder tissues of patients suffering from gallbladder cancer [63]. Taken together with these findings, our results collectively suggest a potential disruption in intracellular copper ion homeostasis within tumor cells. The enrichment observation of the Cup.Sig gene implies its involvement in diverse metabolic functions, thereby providing further evidence for the association between copper homeostasis imbalance and cellular metabolism in malignant cells. Based on our research findings demonstrating a correlation between Cup.Sig scores and immune cell infiltration levels in diverse cancer microenvironments, as well as previous studies highlighting the regulatory effect of copper on the crucial immune checkpoint gene PD-L1 expression [64], we conducted an analysis to assess the predictive impact of Cup.Sig on immunotherapy response. Unlike most studies that indirectly predict immune response through gene expression levels or TIDE scores, we directly utilized immunotherapy cohorts from public databases and evaluated the predictive performance of Cup.Sig using various machine learning algorithms. Our analysis across multiple immunotherapy cohorts consistently demonstrated that Cup.Sig outperformed other signatures in terms of predictive accuracy.

We also developed prognostic risk score based on Cup.Sig and validated the risk scores on multiple platforms and datasets. We identified key genes for predicting pan-cancer OS in Cup.Sig, including *ATOX1*, *CDKN2A*, *CDKN2B-AS1*, *DLD*, *MALAT1*, *KIZ*, *MTTP*, *MYLK*, *NNAT*, *PDHA1* and *PDHB*. In NSCLC, *ATOX1* has been observed to be modulated by the cuproptosis related gene *LIPT1*, leading to its downregulation and subsequently impacting cancer progression [65]. The differential expression of the cuproptosis gene *CDKN2A* has been reported in ccRCC and normal tissues [66], and our study also observed it as a significant prognostic risk factor in ACC, COAD, KICH, LIHC, PCPG, THCA and UCEA. The ceRNA mechanism of *CDKN2B-AS1* promotes the upregulation of the cuproptosis gene *SLC31A1* in breast cancer, and its expression is closely associated with patient prognosis and drug response in this malignancy [67]. The gene *DLD* has also been found to be associated with poor prognosis and malignant biological characteristics in lung adenocarcinoma [68]. *MALAT1* has also been identified as a regulator of the cuproptosis gene *MTF1* through *hsa-miR-32-5p* in the ceRNA network, thereby impacting the pathogenesis and progression of AML [69]. The involvement of *MTTP* in the regulation of metal ion homeostasis in hepatocellular carcinoma also has been well-documented [70]. These results further support the impact of malignant cell cuproptosis on various cancer survival outcomes. In conclusion, these findings collectively underscore the significant importance of cuproptosis in accurately predicting individual patients' survival and treatment response, thereby potentially driving the development of personalized treatment approaches in precision oncology.

There are several limitations in our study that need to be addressed. Firstly, it is imperative to validate the bioinformatics analysis results obtained from single-cell and whole-tissue cancer data by conducting multiple in vivo or in vitro experiments to mitigate potential analytical biases. Moreover, this study solely relies on published transcriptome data, which may not necessarily reflect protein functionality. Furthermore, considering the current scarcity of large-scale pan-cancer proteomic databases, we should expand our research accordingly once access to these proteomic databases becomes available. Through comprehensive analysis of large-scale single-cell and bulk data, we have discovered a robust correlation between cuproptosis and tumor survival, as well as the effectiveness of ICI therapy. Most notably, we have successfully developed a gene expression signature known as Cup.Sig that exhibits remarkable predictive power for immunotherapy response and overall survival outcomes across various cancer types.

5. Conclusions

In conclusion, our findings offer valuable insights into the molecular and cellular mechanisms associated with cuproptosis in malignant cells. Through comprehensive analysis of single-cell transcriptome data across various cancer types, we have successfully identified a distinct gene signature for cuproptosis in malignant cells, denoted as Cup.Sig. From a translational standpoint, the pan-cancer gene signature Cup.Sig established in this study has the potential to enhance prognostic predictions and improve response to immune therapy within the realm of precision oncology.

Funding

This work was supported by the National Natural Science Foundation of China (grant numbers 81673036).

Ethical statement

Review and/or approval by an ethics committee was not needed for this study because it is not involved any human or animal experiments.

Data availability statement

All the data used in this study are publicly available, as described in the Methods section. This paper provides network links or unique identifiers for public queues/datasets.

CRediT authorship contribution statement

Xiaojing Zhu: Writing – original draft, Visualization, Validation, Methodology, Formal analysis, Data curation. **Zixin Zhang:** Methodology, Data curation. **Yanqi Xiao:** Writing – original draft. **Hao Wang:** Writing – review & editing. **Jiaxing Zhang:** Writing – original draft. **Mingwei Wang:** Writing – review & editing, Writing – original draft. **Minghui Jiang:** Writing – review & editing, Writing – original draft. **Yan Xu:** Writing – review & editing, Supervision, Conceptualization.

Declaration of competing interest

The authors declare that they have no known competing financial interests or personal relationships that could have appeared to influence the work reported in this paper.

Abbreviations

SKCM Skin Cutaneous Melanoma
scRNA-seq Single-cell RNA sequencing
Cup.Sig Cuproptosis-related signature
TISCH2 Tumor Immune Single-cell Hub 2
BCC Basal Cell Carcinoma
CRC Colorectal Cancer
CHOL Cholangiocarcinoma
DLBC Diffuse Large B-Cell Lymphoma
ESCA Esophageal Cancer
HNSC Head and Neck Squamous Cell Carcinoma
LIHC Liver Hepatocellular Carcinoma
MCC Merkel Cell Carcinoma
MM Multiple Myeloma
NPC Nasopharyngeal Carcinoma
NSCLC Non-Small Cell Lung Cancer
OV Ovarian Serous Cystadenocarcinom
PAAD Pancreatic Ductal Adenocarcinom
PRAD Prostate Adenocarcinom
LogFC Log-fold change
FDR False discovery rate
TCGA The Cancer Genome Atlas
TMB Total mutation burden
ITH Intratumor heterogeneity
HCC Hepatocellular carcinoma
ICGC International Cancer Genome Consortium
GEO Gene Expression Omnibus
PD-L1 Programmed cell death ligand 1
ICI Immune checkpoint inhibitor
PD-1 Programmed cell death protein 1
CTLA-4 Cytotoxic T lymphocyte-associated antigen 4
CR Complete remission
PR partial remission
SD Stable disease

PD Progressive disease
GO Gene ontology
CIBERSORT Cell-type Identifcation by Estimating Relative Subsets of RNA Transcripts
ESTIMATE The stromal and immune cells within malignant tumor tissues
OS Overall survival
PFI Progression-free interval
DSS Disease-specific survival
AUC Area under curve
LASSO-Cox LASSO penalized Cox proportional hazards regression
EMT Epithelial-mesenchymal transition

Appendix A. Supplementary data

Supplementary data to this article can be found online at https://doi.org/10.1016/j.heliyon.2024.e35404.

References

[1] R.A. Festa, D.J. Thiele, Copper: an essential metal in biology, Curr. Biol. 21 (21) (2011) R877–R883.
[2] P.A. Cobine, S.A. Moore, S.C. Leary, Getting out what you put in: copper in mitochondria and its impacts on human disease, Biochim. Biophys. Acta Mol. Cell Res. 1868 (1) (2021) 118867.
[3] P. Tsvetkov, S. Coy, B. Petrova, M. Dreishpoon, A. Verma, M. Abdusamad, J. Rossen, L. Joesch-Cohen, R. Humeidi, R.D. Spangler, et al., Copper induces cell death by targeting lipoylated TCA cycle proteins, Science 375 (6586) (2022) 1254–1261.
[4] S. Sriskanthadevan, D.V. Jeyaraju, T.E. Chung, S. Prabha, W. Xu, M. Skrtic, B. Jhas, R. Hurren, M. Gronda, X. Wang, et al., AML cells have low spare reserve capacity in their respiratory chain that renders them susceptible to oxidative metabolic stress, Blood 125 (13) (2015) 2120–2130.
[5] P.E. Porporato, N. Filigheddu, J.M.B. Pedro, G. Kroemer, L. Galluzzi, Mitochondrial metabolism and cancer, Cell Res. 28 (3) (2018) 265–280.
[6] L. Sun, Y. Zhang, B. Yang, S. Sun, P. Zhang, Z. Luo, T. Feng, Z. Cui, T. Zhu, Y. Li, et al., Lactylation of METTL16 promotes cuproptosis via m(6)A-modification on FDX1 mRNA in gastric cancer, Nat. Commun. 14 (1) (2023) 6523.
[7] Y. Qin, Y. Liu, X. Xiang, X. Long, Z. Chen, X. Huang, J. Yang, W. Li, Cuproptosis correlates with immunosuppressive tumor microenvironment based on pan-cancer multiomics and single-cell sequencing analysis, Mol. Cancer 22 (1) (2023) 59.
[8] B. Guo, F. Yang, L. Zhang, Q. Zhao, W. Wang, L. Yin, D. Chen, M. Wang, S. Han, H. Xiao, et al., Cuproptosis induced by ROS responsive nanoparticles with elesclomol and copper combined with alphaPD-L1 for enhanced cancer immunotherapy, Adv Mater 35 (22) (2023) e2212267.
[9] X. Huang, S. Zhou, J. Toth, A. Hajdu, Cuproptosis-related gene index: a predictor for pancreatic cancer prognosis, immunotherapy efficacy, and chemosensitivity, Front. Immunol. 13 (2022) 978865.
[10] M. Buccarelli, Q.G. D'Alessandris, P. Matarrese, C. Mollinari, M. Signore, A. Cappannini, M. Martini, P. D'Aliberti, G. De Luca, F. Pedini, et al., Elesclomol-induced increase of mitochondrial reactive oxygen species impairs glioblastoma stem-like cell survival and tumor growth, J. Exp. Clin. Cancer Res. 40 (1) (2021) 228.
[11] Y. Cai, Q. He, W. Liu, Q. Liang, B. Peng, J. Li, W. Zhang, F. Kang, Q. Hong, Y. Yan, et al., Comprehensive analysis of the potential cuproptosis-related biomarker LIAS that regulates prognosis and immunotherapy of pan-cancers, Front. Oncol. 12 (2022) 952129.
[12] L. Jin, W. Mei, X. Liu, X. Sun, S. Xin, Z. Zhou, J. Zhang, B. Zhang, P. Chen, M. Cai, et al., Identification of cuproptosis -related subtypes, the development of a prognosis model, and characterization of tumor microenvironment infiltration in prostate cancer, Front. Immunol. 13 (2022) 974034.
[13] Q. Song, R. Zhou, F. Shu, W. Fu, Cuproptosis scoring system to predict the clinical outcome and immune response in bladder cancer, Front. Immunol. 13 (2022) 958368.
[14] C. Raggi, M.L. Taddei, E. Sacco, N. Navari, M. Correnti, B. Piombanti, M. Pastore, C. Campani, E. Pranzini, J. Iorio, et al., Mitochondrial oxidative metabolism contributes to a cancer stem cell phenotype in cholangiocarcinoma, J. Hepatol. 74 (6) (2021) 1373–1385.
[15] D.S. Matassa, M.R. Amoroso, H. Lu, R. Avolio, D. Arzeni, C. Procaccini, D. Faicchia, F. Maddalena, V. Simeon, I. Agliarulo, et al., Oxidative metabolism drives inflammation-induced platinum resistance in human ovarian cancer, Cell Death Differ. 23 (9) (2016) 1542–1554.
[16] A. Cruz-Bermudez, R. Laza-Briviesca, R.J. Vicente-Blanco, A. Garcia-Grande, M.J. Coronado, S. Laine-Menendez, S. Palacios-Zambrano, M.R. Moreno-Villa, A. M. Ruiz-Valdepenas, C. Lendinez, et al., Cisplatin resistance involves a metabolic reprogramming through ROS and PGC-1 alpha in NSCLC which can be overcome by OXPHOS inhibition, Free Radic. Biol. Med. 135 (2019) 167–181.
[17] J. Xie, Y. Yang, Y. Gao, J. He, Cuproptosis: mechanisms and links with cancers, Mol. Cancer 22 (1) (2023) 46.
[18] Z.R. Jiang, L.H. Yang, L.Z. Jin, L.M. Yi, P.P. Bing, J. Zhou, J.S. Yang, Identification of novel cuproptosis-related lncRNA signatures to predict the prognosis and immune microenvironment of breast cancer patients, Front. Oncol. 12 (2022) 988680.
[19] Y. Zhou, Q. Shu, Z. Fu, C. Wang, J. Gu, J. Li, Y. Chen, M. Xie, A novel risk model based on cuproptosis-related lncRNAs predicted prognosis and indicated immune microenvironment landscape of patients with cutaneous melanoma, Front. Genet. 13 (2022) 959456.
[20] X. Yang, X. Wang, X. Sun, M. Xiao, L. Fan, Y. Su, L. Xue, S. Luo, S. Hou, H. Wang, Construction of five cuproptosis-related lncRNA signature for predicting prognosis and immune activity in skin cutaneous melanoma, Front. Genet. 13 (2022) 972899.
[21] X. Liu, L. Zhou, M. Gao, S. Dong, Y. Hu, C. Hu, Signature of seven cuproptosis-related lncRNAs as a novel biomarker to predict prognosis and therapeutic response in cervical cancer, Front. Genet. 13 (2022) 989646.
[22] Y. Han, Y. Wang, X. Dong, D. Sun, Z. Liu, J. Yue, H. Wang, T. Li, C. Wang, TISCH2: expanded datasets and new tools for single-cell transcriptome analyses of the tumor microenvironment, Nucleic Acids Res. 51 (D1) (2023) D1425–D1431.
[23] Y. Hao, S. Hao, E. Andersen-Nissen, W.M. Mauck 3rd, S. Zheng, A. Butler, M.J. Lee, A.J. Wilk, C. Darby, M. Zager, et al., Integrated analysis of multimodal single-cell data, Cell 184 (13) (2021) 3573–3587 e3529.
[24] X. Jiang, J. Ke, L. Jia, X. An, H. Ma, Z. Li, W. Yuan, A novel cuproptosis-related gene signature of prognosis and immune microenvironment in head and neck squamous cell carcinoma cancer, J. Cancer Res. Clin. Oncol. 149 (1) (2023) 203–218.
[25] M.J. Goldman, B. Craft, M. Hastie, K. Repecka, F. McDade, A. Kamath, A. Banerjee, Y. Luo, D. Rogers, A.N. Brooks, et al., Visualizing and interpreting cancer genomics data via the Xena platform, Nat. Biotechnol. 38 (6) (2020) 675–678.
[26] J. Gao, B.A. Aksoy, U. Dogrusoz, G. Dresdner, B. Gross, S.O. Sumer, Y. Sun, A. Jacobsen, R. Sinha, E. Larsson, et al., Integrative analysis of complex cancer genomics and clinical profiles using the cBioPortal, Sci. Signal. 6 (269) (2013) pl1.
[27] T.X. Huang, L. Fu, The immune landscape of esophageal cancer, Cancer Commun. 39 (1) (2019) 79.
[28] E. Cerami, J. Gao, U. Dogrusoz, B.E. Gross, S.O. Sumer, B.A. Aksoy, A. Jacobsen, C.J. Byrne, M.L. Heuer, E. Larsson, et al., The cBio cancer genomics portal: an open platform for exploring multidimensional cancer genomics data, Cancer Discov. 2 (5) (2012) 401–404.

[29] C. Clarke, S.F. Madden, P. Doolan, S.T. Aherne, H. Joyce, L. O'Driscoll, W.M. Gallagher, B.T. Hennessy, M. Moriarty, J. Crown, et al., Correlating transcriptional networks to breast cancer survival: a large-scale coexpression analysis, Carcinogenesis 34 (10) (2013) 2300–2308.
[30] M. Sheffer, M.D. Bacolod, O. Zuk, S.F. Giardina, H. Pincas, F. Barany, P.B. Paty, W.L. Gerald, D.A. Notterman, E. Domany, Association of survival and disease progression with chromosomal instability: a genomic exploration of colorectal cancer, Proc Natl Acad Sci U S A 106 (17) (2009) 7131–7136.
[31] G. Wichmann, M. Rosolowski, K. Krohn, M. Kreuz, A. Boehm, A. Reiche, U. Scharrer, D. Halama, J. Bertolini, U. Bauer, et al., The role of HPV RNA transcription, immune response-related gene expression and disruptive TP53 mutations in diagnostic and prognostic profiling of head and neck cancer, Int. J. Cancer 137 (12) (2015) 2846–2857.
[32] X.J. Yang, M.H. Tan, H.L. Kim, J.A. Ditlev, M.W. Betten, C.E. Png, E.J. Kort, K. Futami, K.A. Furge, M. Takahashi, et al., A molecular classification of papillary renal cell carcinoma, Cancer Res. 65 (13) (2005) 5628–5637.
[33] C.L. Hsu, D.L. Ou, L.Y. Bai, C.W. Chen, L. Lin, S.F. Huang, A.L. Cheng, Y.M. Jeng, C. Hsu, Exploring markers of exhausted CD8 T cells to predict response to immune checkpoint inhibitor therapy for hepatocellular carcinoma, Liver Cancer 10 (4) (2021) 346–359.
[34] H. Okayama, T. Kohno, Y. Ishii, Y. Shimada, K. Shiraishi, R. Iwakawa, K. Furuta, K. Tsuta, T. Shibata, S. Yamamoto, et al., Identification of genes upregulated in ALK-positive and EGFR/KRAS/ALK-negative lung adenocarcinomas, Cancer Res. 72 (1) (2012) 100–111.
[35] T. Takeuchi, S. Tomida, Y. Yatabe, T. Kosaka, H. Osada, K. Yanagisawa, T. Mitsudomi, T. Takahashi, Expression profile-defined classification of lung adenocarcinoma shows close relationship with underlying major genetic changes and clinicopathologic behaviors, J. Clin. Oncol. 24 (11) (2006) 1679–1688.
[36] F. Baty, M. Joerger, M. Fruh, D. Klingbiel, F. Zappa, M. Brutsche, 24h-gene variation effect of combined bevacizumab/erlotinib in advanced non-squamous non-small cell lung cancer using exon array blood profiling, J. Transl. Med. 15 (1) (2017) 66.
[37] J.K. Stratford, D.J. Bentrem, J.M. Anderson, C. Fan, K.A. Volmar, J.S. Marron, E.D. Routh, L.S. Caskey, J.C. Samuel, C.J. Der, et al., A six-gene signature predicts survival of patients with localized pancreatic ductal adenocarcinoma, PLoS Med. 7 (7) (2010) e1000307.
[38] T.N. Gide, C. Quek, A.M. Menzies, A.T. Tasker, P. Shang, J. Holst, J. Madore, S.Y. Lim, R. Velickovic, M. Wongchenko, et al., Distinct immune cell populations define response to anti-PD-1 monotherapy and anti-PD-1/anti-CTLA-4 combined therapy, Cancer Cell 35 (2) (2019) 238–255 e236.
[39] T. Nathanson, A. Ahuja, A. Rubinsteyn, B.A. Aksoy, M.D. Hellmann, D. Miao, E. Van Allen, T. Merghoub, J.D. Wolchok, A. Snyder, et al., Somatic mutations and neoepitope homology in melanomas treated with CTLA-4 blockade, Cancer Immunol. Res. 5 (1) (2017) 84–91.
[40] D. Liu, B. Schilling, D. Liu, A. Sucker, E. Livingstone, L. Jerby-Arnon, L. Zimmer, R. Gutzmer, I. Satzger, C. Loquai, et al., Integrative molecular and clinical modeling of clinical outcomes to PD1 blockade in patients with metastatic melanoma, Nat Med 25 (12) (2019) 1916–1927.
[41] W. Hugo, J.M. Zaretsky, L. Sun, C. Song, B.H. Moreno, S. Hu-Lieskovan, B. Berent-Maoz, J. Pang, B. Chmielowski, G. Cherry, et al., Genomic and transcriptomic features of response to anti-PD-1 therapy in metastatic melanoma, Cell 165 (1) (2016) 35–44.
[42] E.M. Van Allen, D. Miao, B. Schilling, S.A. Shukla, C. Blank, L. Zimmer, A. Sucker, U. Hillen, M.H.G. Foppen, S.M. Goldinger, et al., Genomic correlates of response to CTLA-4 blockade in metastatic melanoma, Science 350 (6257) (2015) 207–211.
[43] N. Riaz, J.J. Havel, V. Makarov, A. Desrichard, W.J. Urba, J.S. Sims, F.S. Hodi, S. Martin-Algarra, R. Mandal, W.H. Sharfman, et al., Tumor and microenvironment evolution during immunotherapy with nivolumab, Cell 171 (4) (2017) 934–949 e916.
[44] S. Mariathasan, S.J. Turley, D. Nickles, A. Castiglioni, K. Yuen, Y. Wang, E.E. Kadel III, H. Koeppen, J.L. Astarita, R. Cubas, et al., TGFbeta attenuates tumour response to PD-L1 blockade by contributing to exclusion of T cells, Nature 554 (7693) (2018) 544–548.
[45] J. Zhao, A.X. Chen, R.D. Gartrell, A.M. Silverman, L. Aparicio, T. Chu, D. Bordbar, D. Shan, J. Samanamud, A. Mahajan, et al., Author Correction: immune and genomic correlates of response to anti-PD-1 immunotherapy in glioblastoma, Nat Med 25 (6) (2019) 1022.
[46] S.T. Kim, R. Cristescu, A.J. Bass, K.M. Kim, J.I. Odegaard, K. Kim, X.Q. Liu, X. Sher, H. Jung, M. Lee, et al., Comprehensive molecular characterization of clinical responses to PD-1 inhibition in metastatic gastric cancer, Nat Med 24 (9) (2018) 1449–1458.
[47] D.A. Braun, Y. Hou, Z. Bakouny, M. Ficial, M. Sant' Angelo, J. Forman, P. Ross-Macdonald, A.C. Berger, O.A. Jegede, L. Elagina, et al., Interplay of somatic alterations and immune infiltration modulates response to PD-1 blockade in advanced clear cell renal cell carcinoma, Nat Med 26 (6) (2020) 909–918.
[48] G. Yu, L.G. Wang, Y. Han, Q.Y. He, clusterProfiler: an R package for comparing biological themes among gene clusters, OMICS 16 (5) (2012) 284–287.
[49] A.M. Newman, C.L. Liu, M.R. Green, A.J. Gentles, W. Feng, Y. Xu, C.D. Hoang, M. Diehn, A.A. Alizadeh, Robust enumeration of cell subsets from tissue expression profiles, Nat. Methods 12 (5) (2015) 453–457.
[50] W.E. Johnson, C. Li, A. Rabinovic, Adjusting batch effects in microarray expression data using empirical Bayes methods, Biostatistics 8 (1) (2007) 118–127.
[51] M. Ayers, J. Lunceford, M. Nebozhyn, E. Murphy, A. Loboda, D.R. Kaufman, A. Albright, J.D. Cheng, S.P. Kang, V. Shankaran, et al., IFN-gamma-related mRNA profile predicts clinical response to PD-1 blockade, J. Clin. Invest. 127 (8) (2017) 2930–2940.
[52] M. Ju, J. Bi, Q. Wei, L. Jiang, Q. Guan, M. Zhang, X. Song, T. Chen, J. Fan, X. Li, et al., Pan-cancer analysis of NLRP3 inflammasome with potential implications in prognosis and immunotherapy in human cancer, Briefings Bioinf. 22 (4) (2021).
[53] A. Miranda, P.T. Hamilton, A.W. Zhang, S. Pattnaik, E. Becht, A. Mezheyeuski, J. Bruun, P. Micke, A. de Reynies, B.H. Nelson, Cancer stemness, intratumoral heterogeneity, and immune response across cancers, Proc Natl Acad Sci U S A 116 (18) (2019) 9020–9029.
[54] Y. Wang, L. Zhang, F. Zhou, Cuproptosis: a new form of programmed cell death, Cell. Mol. Immunol. 19 (8) (2022) 867–868.
[55] J. Lin, G. Wang, S. Cheng, Y. Hu, H. Li, W. Feng, X. Liu, C. Xu, Pan-cancer analysis of the cuproptosis-related gene DLD, Mediators Inflamm 2023 (2023) 5533444.
[56] C. Deng, Z.X. Li, C.J. Xie, Q.L. Zhang, B.S. Hu, M.D. Wang, J. Mei, C. Yang, Z. Zhong, K.W. Wang, Pan-cancer analysis of CDKN2A alterations identifies a subset of gastric cancer with a cold tumor immune microenvironment, Hum. Genom. 18 (1) (2024) 55.
[57] L. Deng, A. Jiang, H. Zeng, X. Peng, L. Song, Comprehensive analyses of PDHA1 that serves as a predictive biomarker for immunotherapy response in cancer, Front. Pharmacol. 13 (2022) 947372.
[58] W. Wang, X. Wang, J. Luo, X. Chen, K. Ma, H. He, W. Li, J. Cui, Serum copper level and the copper-to-zinc ratio could Be useful in the prediction of lung cancer and its prognosis: a case-control study in northeast China, Nutr. Cancer 73 (10) (2021) 1908–1915.
[59] S.A.K. Saleh, H.M. Adly, A.A. Abdelkhaliq, A.M. Nassir, Serum levels of selenium, zinc, copper, manganese, and iron in prostate cancer patients, Curr. Urol. 14 (1) (2020) 44–49.
[60] V. Pavithra, T.G. Sathisha, K. Kasturi, D.S. Mallika, S.J. Amos, S. Ragunatha, Serum levels of metal ions in female patients with breast cancer, J. Clin. Diagn. Res. 9 (1) (2015) BC25–c27.
[61] M. Yaman, G. Kaya, H. Yekeler, Distribution of trace metal concentrations in paired cancerous and non-cancerous human stomach tissues, World J. Gastroenterol. 13 (4) (2007) 612–618.
[62] F. Kosova, B. Cetin, M. Akinci, S. Aslan, A. Seki, Y. Pirhan, Z. Ari, Serum copper levels in benign and malignant thyroid diseases, Bratisl. Lek. Listy 113 (12) (2012) 718–720.
[63] S. Basu, M.K. Singh, T.B. Singh, S.K. Bhartiya, S.P. Singh, V.K. Shukla, Heavy and trace metals in carcinoma of the gallbladder, World J. Surg. 37 (11) (2013) 2641–2646.
[64] F. Voli, E. Valli, L. Lerra, K. Kimpton, F. Saletta, F.M. Giorgi, D. Mercatelli, J.R.C. Rouaen, S. Shen, J.E. Murray, et al., Intratumoral copper modulates PD-L1 expression and influences tumor immune evasion, Cancer Res. 80 (19) (2020) 4129–4144.
[65] R. Deng, L. Zhu, J. Jiang, J. Chen, H. Li, Cuproptosis-related gene LIPT1 as a prognostic indicator in non-small cell lung cancer: functional involvement and regulation of ATOX1 expression, Biomol Biomed 24 (3) (2024) 647–658.
[66] Z. Bian, R. Fan, L. Xie, A novel cuproptosis-related prognostic gene signature and validation of differential expression in clear cell renal cell carcinoma, Genes 13 (5) (2022).
[67] X. Li, Z. Ma, L. Mei, Cuproptosis-related gene SLC31A1 is a potential predictor for diagnosis, prognosis and therapeutic response of breast cancer, Am. J. Cancer Res. 12 (8) (2022) 3561–3580.

[68] X. Li, J. Rui, Z. Yang, F. Shang-Guan, H. Shi, D. Wang, J. Sun, Cuproptosis related gene DLD associated with poor prognosis and malignant biological characteristics in lung adenocarcinoma, Curr. Cancer Drug Targets. 24 (8) (2024) 867–880.
[69] Y. Li, X. Kan, Cuproptosis-related genes MTF1 and LIPT1 as novel prognostic biomarker in acute myeloid leukemia, Biochem. Genet. 62 (2) (2024) 1136–1159.
[70] Z. Liu, H. Ma, Z. Lai, The role of ferroptosis and cuproptosis in curcumin against hepatocellular carcinoma, Molecules 28 (4) (2023).